Forced convection heat transfer from an elliptic cylinder placed in focus of a parabolic solar concentrator

M. S. Mostafa, R. M. Kamal and M. H. Gobran
Mechanical Power Eng. Dept., Faculty of Eng., Zagazig University, Zagazig, Egypt

An experimental investigation has been made to clarify the heat transfer characteristics around an elliptic cylinder placed in focus of a parabolic concentrator. The elliptic cylinder examined, has an axis ratio 1:2.17 and a parabolic concentrator with rim angle 90° has been used. The testing fluid was air and the Reynolds number based on the major axis length, c ranged from about 5×10^3 to 3×10^4. The angle of attack was changed from 0° to 90° at 15° interval. It is found that the local heat transfer features are, in general, independent of the Reynolds number, and their values are different from those of a cylinder/plate combination. Over the Reynolds number range examined, the values of Nu_m at $a = 75°$ and 90° are nearly equal to each other and are the highest. For free cylinder, Nu_m is lowest at $a = 30°$ but for cylinder/plate combination, Nu_m is lowest at $a = 0°$. There is no essential change in the values of Nu_m in the range of $a = 0°$ to 15°. The values of Nu_m for free cylinder are higher than those for cylinder/plate combination at all angles of attack and Reynolds number range examined. The value of mean Nusselt number for free cylinder and cylinder/plate combination can be calculated from the following equation; $Nu_m = a\, Re^m\, [1 - n\cos\alpha]$ with maximum percentage error ± 11.8 % for free cylinder and ± 8.5 % for cylinder/plate combination.

فى المركزات الشمسية يتم حساب معامل انتقال الحرارة حول الأسطوانة الدائرية الموضوعة فى بؤرة المركز مـــن العلاقـــة المعروفة و المعطاة بواسطة هلبرت (١٩٣٣) و تختلف القيم المعطاة بواسطة هلبرت عن القيم الفعلية نظرا لاختلاف طبيعة سريان المائع حول الاسطوانة فى حالة المركزات الشمسية و لا يختلف الحال بالنسبة للاسطوانة بيضاوية الـــشكل. و بنـــاءا على ذلك فقد تم عمل دراسة معملية لدراسة تأثير وجود حائل على شكل قطع مكافئ ذو زاوية حـرف ٩٠ درجة خلـف اسطوانة بيضاوية الشكل نسبة قطرها الأصغر الى الأكبر ١ : ٢,١٧ على معامل انتقال الحـــرارة الموضـــعى و المتوسـط حول سطح الاسطوانة، و تم استخدام الهواء كمائع للدراسة و قد تراوح رقم رينولدز بين ٥,٥ x ١٠ ³ الى ٣ x ١٠ ٤ و قد تمت مقارنة خصائص انتقال الحرارة حول الاسطوانة المنفردة بخصائصه فى حالة وجودها فى بؤرة الحائـــل عنـــد زوايـــا سقوط مختلفة. و قد وجد أن شكل معامل انتقال الحرارة حول سطح الاسطوانة لا يعتمد على رقم رينولدز ، و معامل انتقال الحرارة المتوسط يزداد بزيادة زاوية السقوط و يبلغ قيمته القصوى عند زاوية سقوط ٧٥ و ٩٠ درجة و أقل قيمة لـــه عنـــد زاوية سقوط ٣٠ درجة بالنسبة للاسطوانة المنفردة و صفر و ١٥ درجة بالنسبة للاسطوانة الموضوعة فى بــؤرة الحائـل، هذا و قد لوحظ أن قيم معامل انتقال الحرارة المتوسطة للاسطوانة المنفردة أكبر منه فى حالة الاسطوانة و الحائل، و قد تـــم استنباط معادلة رياضية تربط بين معامل انتقال الحرارة المتوسط و رقم رينولدز و زاوية السقوط و قد وجـــد تطـــابق بـــين النتائج المعملية و القيم المحسوبة بواسطة تلك المعادلة بنسبة خطأ قصوى ١١,٨ % بالنسبة للاسطوانة المنفـــردة و٨,٥ % بالنسبة للاسطوانة الموضوعة في بؤرة الحائل.

Keywords: Convective heat transfer, Forced convection, Experimental study, Elliptic cylinder, Parabolic concentrator

1. Introduction

For the purpose of saving energy and making its use effective, it is very important to exploit high performance solar concentrators. The overall performance of solar concentrators depends on energy losses. Energy losses for solar concentrators are optical losses and thermal losses.

The useful energy gain can be maximized if all losses are minimized.

The thermal losses are classified as convection losses and radiation losses. For heat lost by convection the convective film coefficient is a strong function of the external flow conditions in the vicinity of the envelope of the absorber element.

As far as the heat transfer characteristics of the elliptic cylinders are concerned, there

have been only a few investigations. Boundary layer analyses were made by Chao et al. [1]. Their results naturally may be applicable only to the upstream surface of the elliptic cylinder on which a laminar boundary layer develops. Seban et al. [2] and Drake et al. [3] measured the local heat transfer coefficient on elliptic cylinders of axis ratios 1:4 and 1:3 respectively. Their main purpose, however seemed to confirm the applicability of the boundary layer theory. The angle of attack examined by them was limited to 0, 5, and 6 deg, and the mean heat transfer coefficient was not measured. Ota et al. [4-5] have conducted experimental studies of forced convection heat transfer from elliptic cylinders of axis ratio 1:2 and 1:3. The local heat transfer features are clarified and it is found that they are quite different from those of the circular cylinder. The mean heat transfer coefficient depends upon the axis ratio, the angle of attack, and the Reynolds number, and it is comparable to or higher than that of the circular cylinder over the Reynolds number range studied. Ota et al. [6-7] have conducted an experimental investigation to clarify heat transfer characteristics from two and four elliptic cylinders having an axis ratio 1:2 arranged in tandem in a uniform flow of air. The angle of attack was varied from 0° to 90° and the nondimensional cylinder spacing from 1.25 to 4. They found that the heat transfer features vary drastically with the angle of attack and also with the cylinder spacing. Mostafa [8] carried out an experimental investigation to study the effect of plate geometry and gap ratio on the fluid flow and heat transfer characteristics around a heated circular cylinder. The cylinder was placed at various distances in front of a plate with different geometries (flat or curved plate). He found that the flow patterns and heat transfer characteristics have a strong dependency on the plate geometry and gap ratio.

The present authors have conducted an experimental investigation to study the flow characteristics around an elliptic cylinder placed in the focus of a parabolic plate [9]. Also, they carried out a flow visualization to clarify the flow patterns around the cylinder. An elliptic cylinder with axis ratio 1:2.17, and a parabolic plate with rim angle 90° and

aspect ratio of 1.5 were used. The angle of attack was changed from 0° to 90° at 15° intervals. It was found that the pressure distribution depends strongly upon the angle of attack. For the cylinder/plate combination the form drag increases with α but its value is lower than that of cylinder alone. The location of separation point on the suction side of the cylinder shifts towards the leading edge at $a = 0°$ and 15° compared with that in the case of cylinder alone. Also as the angle of attack increases the flow on the pressure side separates earlier than that of cylinder alone.

For solar concentrator, the convective heat transfer coefficient on the outside surface of circular envelop is usually calculated using the well known correlation based on the data of Hilpert [10]. The values of heat transfer coefficient predicted by Hilpert differ from the actual values in the case of the solar concentrators due to the existence of the reflecting surface near the envelop. For some practical applications an elliptic cylinder was placed in the focus of a parabolic plate, as in the case of solar concentrators. The wind flow around the absorber tube (elliptic or circular cylinder) in this case is more complicated than that in the free cylinder case. Studying the characteristics of heat transfer around an elliptic cylinder placed in the focus of parabolic solar concentrators is important. According to the relevant literature to the authors, pervious studies directly related to this aspect are almost not existing.

The main purpose of the present study is to clarify the local and overall heat transfer characteristics from an elliptic cylinder of axis ratio 1:2 placed in the focus of parabolic concentrator over a relatively wide range of Reynolds number. The angle of attack is varied from 0° through 90°. The flow configuration examined shown in fig. 1, includes the coordinate system employed.

2. Experimental test rig

Measurements were conducted in a low speed wind tunnel discharging air to the atmosphere [8]. The tunnel has a test section of 0.44 x 0.44 m and a length of 1.0 m. During the experiments the flow upstream of the cylinder had uniform velocity profile within
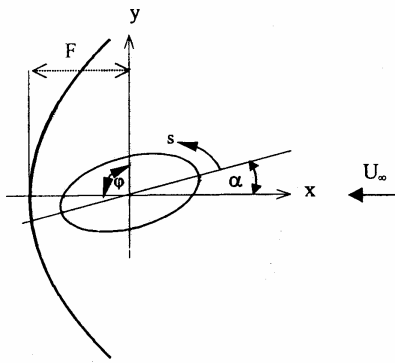
Fig. 1. Cylinder / plate combination.

±1% of the mean value. The velocity at the entrance of the test section (U_∞) was measured by means of a Pitot tube. The uncertainty in the measured velocity was about ± 0.83 %. The experiments were carried out in the subcritical Reynolds number range ($5.5 \times 10^3 \leq Re \leq 3 \times 10^4$).

2.1. Test model

The test model consists of an elliptic cylinder and parabolic plate with a rim angle of 90°. The elliptic cylinder examined has an axis ratio of 1:2.17, the major axis being 27.6 mm and a span length of 440 mm. The cylinder was made of wood by the following procedure. An elliptic edge cutter tool with major axis of 28 mm and 14 mm minor axis was used to shape the wooden cylinder. Finally the cylinder surface was manually finished. Twenty-four copper-constantan thermo-couples of 0.4 mm diameter were embedded on the surface of the elliptic cylinder in order to measure the wall temperature. Finally a nickel-chrome sheet of 0.2 mm thickness and 40 mm width was wound helically and stuck on the cylinder surface as a heating plate. The nickel chrome sheet is divided into three pieces. The mid piece is the active element for the measurements of the local heat transfer. The active element is flanked by two guard pieces, which are used to eliminate the end losses and wall effect (see fig. 2). The cylinder was located horizontally at mid height of the test section in the focal plane of the parabolic plate. The surface distance, *s*, is measured from the leading edge of the cylinder, and it

has a positive sign along the suction side and negative sign along the pressure side. The parabolic plate was made of Plexiglass (120mm width and 6 mm thickness) with aspect ratio of 1.5. The profile of the parabola and the focal property can be obtained using the following equations:

$$x = \frac{y^2}{4F}, \qquad (1)$$

$$F = \frac{H}{2 \sin \varphi}(1 + \cos \varphi) \quad . \qquad (2)$$

Where *x, y* are the coordinates of the parabolic plate, see also table 1.

Heating of the cylinder surface was conducted by means of electric current to the nickel chrome sheet under the condition of constant heat flux. The heat loss by radiation was neglected in the following results. The supplying heat flow rate was determined from the measured power. The heat transfer coefficient and the corresponding Nusselt number are defined as:

$$h = q / (T_w - T_\infty) \quad and \quad Nu = hc/ k.$$
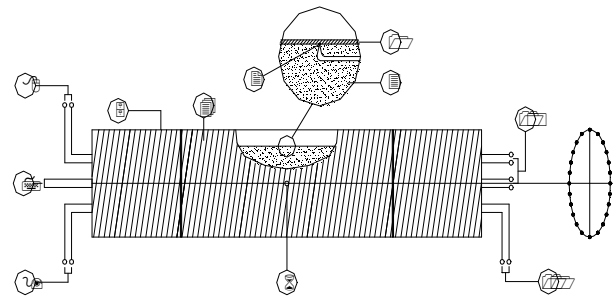
1- Nickel-chrome foil	7- Stainless steel tube
2-Thermocouple junction	8- Thermocouple leads
3-Wooden tube	9- A.C. power leads for main hearter
4- Main heater	10- A.C. power leads for guard heater
5-Guard heater	11- Thermocouple leads
6- Pressure tap	

Fig. 2. Details of heated cylinder.

Table 1
Geometrical characteristics of parabolic plates

W/c	H/c	φ	W/H	(F/c)
8.295	5.529	90°	1.5	2.765

In operating the system, about one hour was required to attain a steady state. In the case of a high Reynolds number q was kept at about 1.4 kW/m², but at a low Reynolds number it was decreased to about 0.3 kW/m² in order to minimize the effects of natural convection.

4. Results and discussion

4.1. Local heat transfer

Fig. 3 illustrates the local Nusselt number distribution along the cylinder surface for different angles of attack (0º to 90º at 15º interval) at various Reynolds numbers. Also the case of free cylinder is shown.

Fig. 3-a represents the local Nusselt at α= 0º. It is clear that the symmetry of the local heat transfer distribution on the upper and lower surfaces is satisfactory at all values of Reynolds number.

Nu attains the highest value at the leading edge and decreases steeply with development of a laminar boundary layer on the upstream face. In separated flow region, Nu again increases in the downstream direction and reaches a maximum at the trailing edge. However Nu shows no essential change therein at very low Reynolds number. This may be due to a very stagnant flow in the near wake.

At α = 15º, the flow is accelerated very rapidly around the leading edge, producing a very steep decrease of Nusselt number on the upper side compared to the lower side as found in fig. 3-b. It is of interest to note that there exists a region where Nu shows little change just behind the separation point on the upper and lower sides especially at low Reynolds numbers for cylinder/plate combination.

Figs. 3-c to 3-g show that, there is unsymmetry of the Nusselt number distribution on the upper and lower sides. It can be seen that with an increase of angle of attack the maximum value of Nusselt number shifts from the leading edge of the cylinder to a point on the lower surface of the cylinder up to a = 45º. This is due to the front stagnation point shift on lower surface of the cylinder with increasing the angle of attack. For a > 45º the maximum value of Nusselt number occurs on the upper surface of the cylinder in the separated flow region, due to mixing associated with vortex formation in the wake of the cylinder. Comparing the results at a = 30º and 45º, it can be seen that in the range of a > 30º, the heat transfer coefficient in the separated flow region is larger than that on the upstream surface where the boundary layer develops. This may be due to the fact that the wake width behind the cylinder increases with the angle of attack.

Needless to say, the local heat transfer coefficient distribution varies with the angle of attack. Fig. 3 reveals that increasing the angle of attack the maximum value of Nusselt number shifts from the leading edge. Also it can be seen that, in the case of cylinder/plate combination the values of local heat transfer coefficient around the cylinder surface are smaller than those around the cylinder surface alone at all Reynolds numbers. This can be explained as follows: when the plate is placed normally in a uniform stream a stagnation region is created on its frontal face. Therefore, the flow within the gap between the cylinder and plate becomes nearly stagnant, [9]. This leads to a decrease in the heat transfer coefficient. The flow pattern around the elliptic cylinder and cylinder/plate combination was visualized at various angles of attack by the present authors [9]. It was found that the position of the upstream stagnation point shifts with a. Also the wake width increases with increasing the angle of attack.

4.2. Mean heat transfer

The mean Nusselt number Nu_m over the whole circumference of the elliptic cylinder was estimated by using numerical integration. The mean Nusselt number is calculated from the following equation:

$$Nu_m = \frac{h_m c}{k} \quad , \tag{3}$$

$$h_m = \frac{1}{B} \int_0^B h \, ds \ . \tag{4}$$

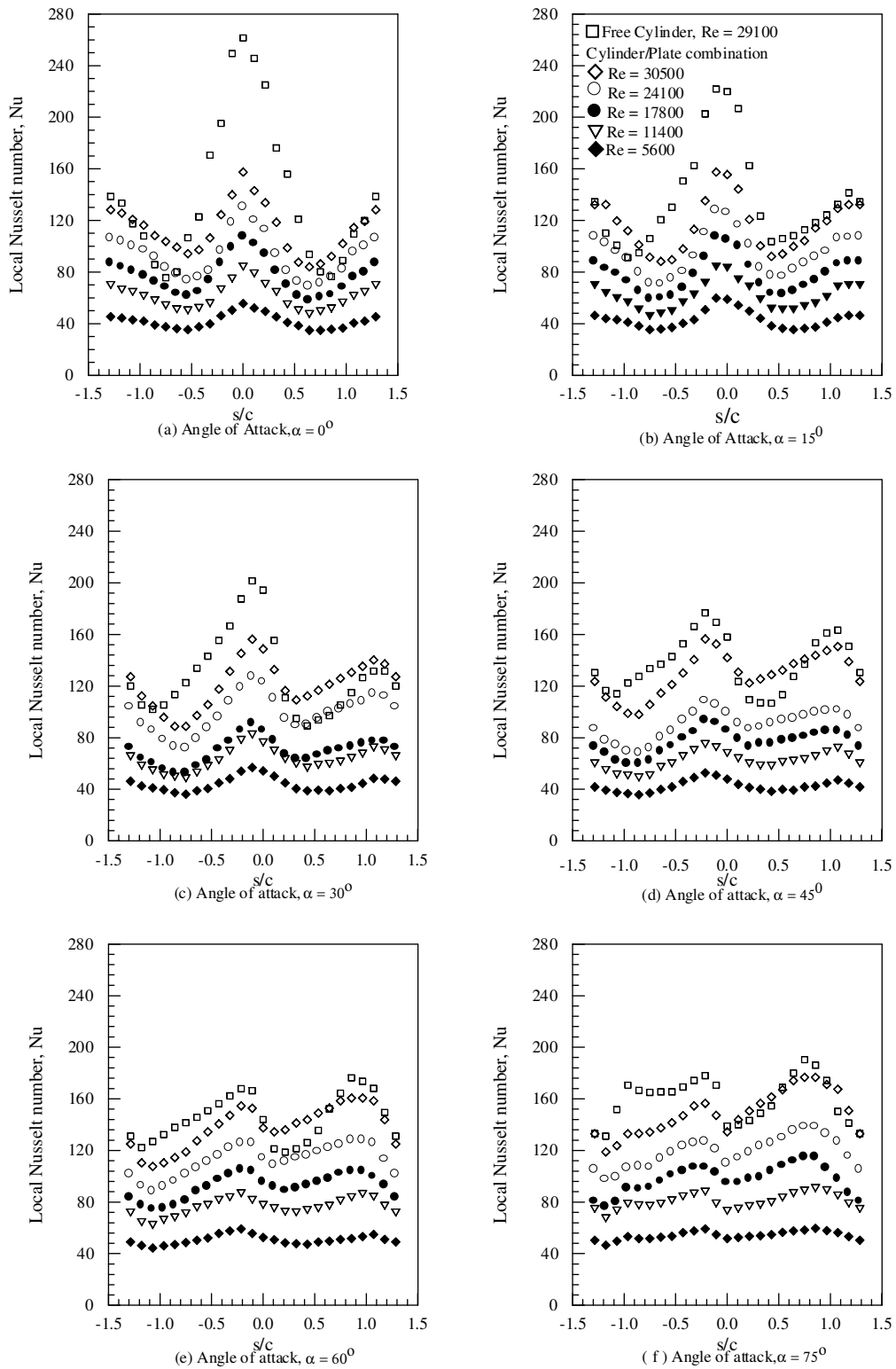Fig. 4 illustrates the variation of Nu_m with α. It can be seen that in the low Reynolds

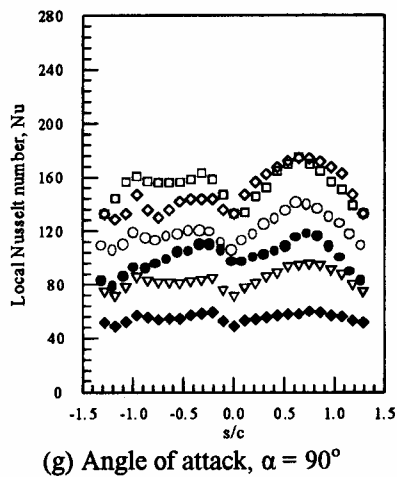Fig. 3. Variation of local Nusselt number with angle of attack at different Reynolds number.

(g) Angle of attack, α = 90°

Fig. 3. Continued.

Fig. 4. Variation of means Nusselt number with angle of attack.

number range of about Re < 11300 for single cylinder and Re < 24100 for cylinder/plate combination, no essential change in the region of α = 0° to 30°. Beyond α = 30°, Nu_m increases slightly with α. On the other hand, in the region of Re ≥ 11300 for single cylinder Nu_m decreases with α in 0° < α < 30°, reaching a minimum around α = 30°, and subseqently increases with α. The mean heat transfer coefficient attains a maximum at α in the range 75° ≤ α ≤ 90° for all values of Reynolds number studied. For cylinder/plate combination in the region Re ≥ 24100 Nu_m increases with α.

Fig. 5 shows the variation of Nu_m with Reynolds number at α = 0°. It can be seen that the values of Nu_m for free cylinder are in a good agreement with Ota work [5]. Also the values of mean Nusselt number for cylinder/plate combination are lower than those of free cylinder by about 15%. This is due to the stagnation region in the gap between the cylinder and plate. The relation between Nu_m and Re for all angles of attack is presented in fig. 6 for cylinder / plate combination. It is clear that as the Reynolds number increases the value of Nu_m increases for all angles of attack. This is due to the decrease in the boundary layer thickness in the leading edge zone, and strong mixing of fluid in the separated region.

It can be seen that as the angle of attack increases in the range 30° ≤ α ≤ 60° the value

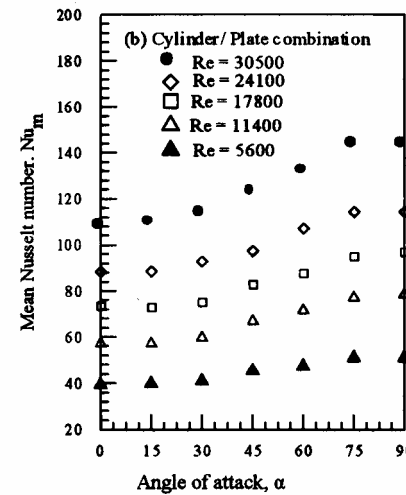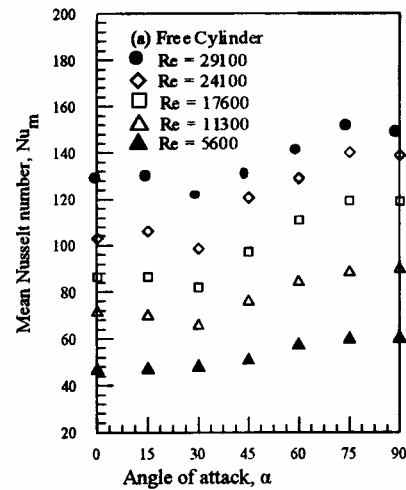of Nu_m increases. This is due to increase of the wake width in the separated region [10]. At α = 0° and 15°, and at α = 75° and 90° the values of Nu_m are identical at all Reynolds numbers.

4.3. Correlation between the Nu_m and angles of attack

It is clear that the mean Nusselt number depends on the Reynolds number and angles of attack. A trial is made to correlate these parameters and a general empirical formula is obtained in the form:

$$Nu_m = a\,Re^{m}[1 - n\cos\alpha]\,. \tag{5}$$

The values a, m, and n are listed in table 2 for free elliptic cylinder and cylinder/plate combination.

Fig. 7 shows a comparison between the experimental results and those calculated from the empirical equation. It can be seen
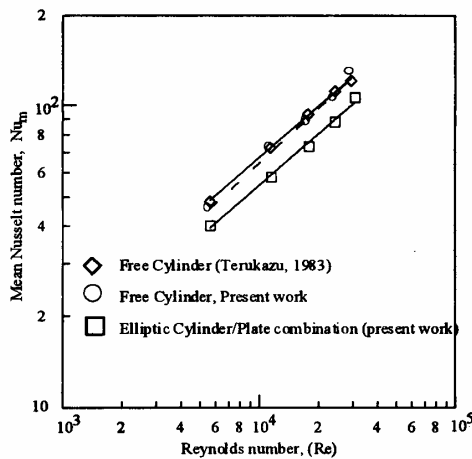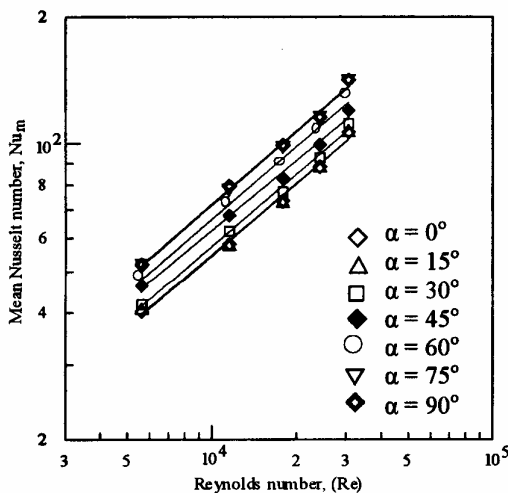

Fig. 5. Mean Nusselt number at $\alpha = 0°$.

Fig. 6. Effect of angle of attack on mean Nusselt number for cylinder/plate combination.

Table 2
Values of a, m, and n

	a	m	n
Free cylinder	0.452	0.571	0.254
Cylinder/plate combination	0.339	0.584	0.246

that the experimental results are in a good agreement with those calculated from the empirical eq. 5 within 11.8% for free cylinder and 8.5% for cylinder/plate combination (maximum percentage error).

5. Concluding remarks

Heat transfer characteristics of an elliptic cylinder having an axis ratio 1:2.17 and cylinder/plate combination are clarified through wind tunnel experiments. The Reynolds number range examined is from about 5.5×10^3 to 3×10^4 and the angle of attack is varied from 0° to 90°. It has been found that:

(i) The local heat transfer features of free cylinder are, in general, independent of the Reynolds number, and are different from those of a cylinder/plate combination.

(ii) The dependency of the mean heat transfer coefficient upon the Reynolds number and angle of attack is clearly recognized. Over the Reynolds number range examined the values of Nu_m at $\alpha = 75°$ and 90° are nearly equal to each other and are the highest. For free cylinder, Nu_m is lowest at $\alpha = 30°$ but for cylinder/plate combination, Nu_m is lowest at $a = 0°$. No essential change in the values of Nu_m is observed in the range of $0° \le \alpha \le 15°$.

(iii) The values of Nu_m for free cylinder are higher than that for cylinder/plate combination at all angles of attack and Reynolds number range examined.

(iv) The value of mean Nusselt number for free cylinder and cylinder/plate combination can be calculated from the following equation;

$$Nu_m = a\,Re^{m}[1 - n\cos\alpha]\,,$$

with maximum percentage error ± 11.8 % for free cylinder and ± 8.5 % for cylinder/plate combination.

Fig. 7. Correlation of mean Nusselt number with Reynolds number as a function of angle of attack.

ρ free stream density.

References

[1] B. T. Chao, and R. O Fagbenle, "on Merk's Method of Calculating Boundary Layer Transfer," Int. J. heat mass transfer, Vol. 17, pp. 223-240 (1974).

[2] R. A. Seban and R. M. Drake, "Local Heat Transfer Coefficients on the Surface of an Elliptic Cylinder in a High Speed Air Flow," Trans. ASME, Vol. 75, pp. 235-240 (1953).

[3] R. M. Drake, R. A. Seban, D. L Doughty, and S. Levy, "Local Heat Transfer Coefficient on Surface of an Elliptic Cylinder, Axis Ratio 1:3, in a High Speed Air Flow," Trans. ASME, Vol. 75, pp. 1291-1302 (1953).

[4] T. Ota, S. Aiba, T. Tsuruta, and M. Kaga, "Forced Convection Heat Transfer From an Elliptic Cylinder of Axis Ratio 1:2," Bull JSME, Vol. 26, pp. 262-267 (1983).

[5] T. Ota, H. Nishiyama, and Y. Taoka, "Heat Transfer and Flow Around an Elliptic Cylinder," Int. J. Heat Mass Transfer, Vol. 27, pp. 1771-1779 (1984).

[6] T. Ota, and H. Nishiyama, "Flow Around Two Elliptic Cylinders in Tandem Arrangement," Trans. ASME, J. fluid Eng., Vol. 108 (1), pp. 98-103 (1986).

[7] T. Ota, H. Nishiyama, J. Kominami, and K. Sato, "Heat Transfer From Two Elliptic Cylinders in Tandem Arrangement," Trans. ASME, J. heat Transfer, Vol. 108 (3), pp. 252-531 (1986).

[8] M. S. Mostafa, Experimental Investigation of Fluid Flow and Heat Transfer Around Circular Cylinder-Flat and Curved Plates Combinations, Ph.D. Thesis, Mechanical Power Engineering, Faculty of Engineering, Cairo University (1998).

[9] M. S. Mostafa, R. M. Kamal, and M. H. Gobran, " Flow Characteristics Around an Elliptic Cylinder Placed in the Foucs of a Parabolic Solar Concentrator of 90° Rim Angle," Alexandria Eng. J., Vol. 40 (1), pp. 9-18 (2001).

[10] R. Hilpert, Geb. Forsch. Ingenieurwes. Vol. 4, p. 215 (1933).

Nomenclature

B	circumference of elliptic cylinder, mm
C	major axis of elliptic cylinder, mm
F	focal length, mm
H	height of parabolic plate, mm
h	heat transfer coefficient, W/m². °C
h_m	mean heat transfer coefficient, W/m².°C
k	thermal conductivity, W/m. °C
Nu	local Nusselt number = h c/ k
Nu_m	mean nusselt number = h_m c / k
q	heat flux, W/m²
Re	Reynolds number = ρU_∞ c/ μ
S	surface distance from leading edge, mm
T_w	wall temperature, °C
T_∞	free stream temperature, °C
U_∞	Free stream velocity,
W	parabolic plate width, mm
x, y	General coordinates,
α	angle of attack,
φ	rim angle,
μ	free stream dynamic viscosity, and